ac electrokinetic phenomena over semiconductive surfaces: Effective electric boundary conditions and their applications

Cunlu Zhao and Chun Yang*

School of Mechanical and Aerospace Engineering, Nanyang Technological University 50 Nanyang Avenue, Singapore 639798, Republic of Singapore

(Received 19 October 2009; revised manuscript received 30 October 2010; published 9 June 2011)

Electrokinetic boundary conditions are derived for ac electrokinetic phenomena over leaky dielectric (i.e., semiconducting) surfaces. Such boundary conditions correlate the electric potentials across a semiconductor-electrolyte interface (consisting of an electric double layer inside the electrolyte solution and a space charge layer inside the semiconductor) in an ac electric field with arbitrary wave forms. The presented electrokinetic boundary conditions allow for evaluation of the induced ζ potential contributed by both bond charges (due to electric polarization) and free charges (due to electric conduction) from the leaky dielectric materials. Two well-known limiting cases, (i) the conventional insulating boundary condition and (ii) the perfectly polarizable boundary condition, can be recovered from the generalized electrokinetic boundary conditions derived in the present paper. Subsequently, we demonstrate the implementation of the derived boundary conditions for analyzing the ac induced-charge electrokinetic flow around a semiconducting cylinder. The results show that the flow circulations exist around the semiconducting cylinder and become stronger in the ac field with a lower frequency and around the semiconducting cylinder with a higher conductivity.

DOI: 10.1103/PhysRevE.83.066304 PACS number(s): 47.57.jd, 47.61.Fg

I. INTRODUCTION

ac electrokinetic (ACEK) phenomena are widely used for manipulations of particles and flows in microfluidic systems [1–3]. The classic description of electrokinetic phenomena relies on the electric double layer (EDL) formed on a charged insulating surface whose surface charge density is fixed due to the physiochemical bonds. Consequently, the surface charge density is independent of the externally applied electric field. However, for electrokinetic phenomena around polarizable or conducting solids, it has been demonstrated that, in the presence of an external electric field, extra electric charges can be induced on polarizable or conducting solid surfaces immersed in an electrolyte solution, thereby triggering the charging of EDL inside the electrolyte solution. This is manifested in a ζ potential, which is no longer a fixed equilibrium material property but rather depends on the external electric field. These induced-charge electrokinetic (ICEK) phenomena were studied for polarizable colloidal particles [4,5] almost two decades ago and recently were studied in the context of microfluidic applications for pumping [6,7], mixing [6,8,9], demixing [10], focusing [11], and particle manipulations [12,13]. All of these studies focused on ICEK phenomena around conductors with ideal polarizability.

Recently, attention has been paid to ICEK phenomena over dielectric surfaces with finite polarizability, and the induced ζ potential, in this case, is solely contributed by the bond charges due to the electric polarization. Squires and Bazant [6] predicted a decrease in the induced ζ potential due to the presence of a thin dielectric coating on a conducting surface. For solids with arbitrary polarizability, two effective electric boundary conditions of a Robin-type and a Neumann-type were derived by Yossifon *et al*. [14] and Zhao and Yang [15] by using different methodologies. These derived effective electric boundary conditions are required for determining the induced ζ potential on an arbitrarily polarizable dielectric surface. Yossifon *et al*. [16] further derived the transient version of these effective boundary conditions, which were used for analyzing the temporary evolution of dc driven electrokinetic phenomena around a polarizable object. Recently, Pascall and Squires [17] experimentally verified that the very presence (often inevitable) of thin dielectric layers on electrode surfaces (e.g., due to surface contamination by oxidized or adsorbed species) can substantially alter the induced ζ potential and, thus, can affect the associated electrokinetic phenomena.

However, aforementioned studies all assumed that the solids were perfectly dielectric, and, thus, there were no free charge carriers and space charge layers (SCLs) inside them. From a more general viewpoint, a solid can have both finite dielectric constant and conductivity and is leaky dielectric or semiconductive in nature. In this circumstance, the SCL forms in the solid, and the EDL forms in the electrolyte liquid, and these two layers constitute the interface between a semiconductor and an electrolyte solution. On the other hand, ac electric field is more desirable in microfluidic applications since it introduces another control parameter of frequency and also reduces possible negative effects, such as electrolysis and dissolution of electrodes. Therefore, this paper presents electrokinetic boundary conditions for ACEK phenomena to correlate the electrical potentials across the EDL and the SCL at a semiconductor-electrolyte solution interface. Such general electrokinetic boundary conditions allow for determining induced ζ potentials on the surface of semiconducting solids subjected to an ac electric field of arbitrary wave forms. Furthermore, the derived electrokinetic boundary conditions are implemented for analyzing the ACEK phenomena around a semiconducting cylinder.

II. EFFECTIVE ELECTRIC BOUNDARY CONDITIONS

It is known that there is usually a SCL (i.e., an EDL in the solid) in the semiconducting solid adjacent to the EDL in the

*mcyang@ntu.edu.sg

liquid electrolyte [18–21]. The thicknesses of EDL and SCL have the same order of magnitude and typically range from 1 to 100 nm, and, thus, both of them need to be considered simultaneously. Then, we need to model the transport (by diffusion and migration) of both types of charge carriers (i.e., electrons and holes) in the solid as what we usually do for both cations and anions in the liquid. We restrict our analysis under the following three assumptions: (i) thin EDL and SCL, (ii) negligible Peclet number, and (iii) small induced electric field [i.e., $\Psi = ze\Phi_0/(k_BT) \ll 1$, wherein z denotes the valence of charge carriers inside the electrolyte solution, e denotes the elemental charge, k_B is the Boltzmann constant, and T is the absolute temperature]. These assumptions were also made in previous studies [6,16,22]. The thin EDL and SCL assumption requires that the EDL thickness and the SCL thickness are much smaller than the characteristic dimension of the semiconductive solid wall a, that is, $\delta_1 = \lambda_{D1}/a \ll 1, \delta_2 = \lambda_{D2}/a \ll 1$. The EDL thickness for a symmetric electrolyte (z:z) can be defined as $\lambda_{D1} = \sqrt{\varepsilon_0\varepsilon_f k_BT/(2n_{01}z^2e^2)}$, and the SCL thickness is similarly defined as $\lambda_{D2} = \sqrt{\varepsilon_0\varepsilon_w k_BT/(2n_{02}e^2)}$, where n_{0i} denotes the bulk concentration of charge carriers inside the liquid and solid domains ($i = 1$ for the electrolytic solution and $i = 2$ for the semiconductor, this convention is complied with in the whole paper), ε_0 is the electric permittivity of vacuum. ε_f and ε_w are the dielectric constants of the electrolyte and the semiconductor, respectively.

From a microfluidic application viewpoint, the aforementioned three assumptions are valid. Therefore, in the model development, the hydrodynamic problem and the electrostatic problem can be decoupled [6,16,22,23]. Furthermore, as shown in Fig. 1, the electrostatic problem can be divided into four subdomains: the two domains for the electroneutral bulk solid wall and bulk solution with their harmonic dimensionless electric potentials Φ_w and Φ_f, respectively, and the two inner domains of the EDL and the SCL whose dimensionless electric potentials, Φ_{EDL} and Φ_{SCL}, should satisfy Poisson's equation. Note that all these dimensionless potentials are scaled with respect to the reference potential Φ_0. To obtain

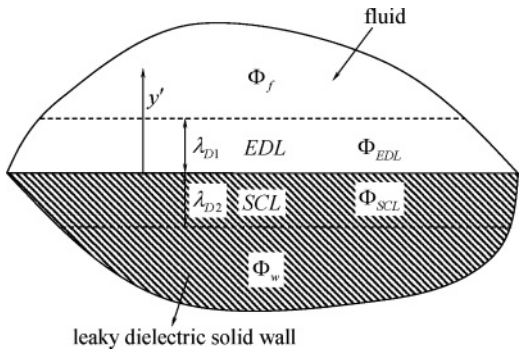

FIG. 1. Aschematic of the electrostatic problem in four subdomains, namely, (i) the bulk electrolyte fluid domain Φ_f, (ii) the bulk leaky dielectric solid wall domain Φ_w, (iii) the EDL domain Φ_{EDL} inside the liquid, and (iv) the SCL domain Φ_{SCL} inside the solid. The dashed lines inside the electrolyte fluid and solid wall, respectively, represent the outer edges of the EDL and SCL where Φ_{EDL} matches Φ_f and Φ_{SCL} matches Φ_w. λ_{D1} and λ_{D2} denote the thicknesses of EDL and SCL, respectively.

the requisite electrokinetic conditions connecting Φ_w and Φ_f on the semiconducting solid-electrolyte interface, we focus on the inner domains, which (for $\delta_1 \ll 1$ and $\delta_2 \ll 1$) is locally one dimensional in the direction of the y' axis, namely, outward normal to the solid surface. We define the corresponding outer (y) and inner (Y_1, Y_2) dimensionless spatial variables through $y' = ay = \lambda_{D1}Y_1 = \lambda_{D2}Y_2$.

In our analysis, the dimensionless net charge densities inside the liquid and solid domains due to the difference between the concentration of positive charge carriers and that of negative charge carriers, i.e., $n_p - n_n$, is expressed as $\rho_i = (n_{pi} - n_{ni})/(2\Psi n_{0i})$. For the leading order (in the limit of small δ_1, δ_2, and Ψ), Φ_{EDL} and Φ_{SCL}, respectively, satisfy Poisson's equations,

$$\frac{\partial^2\Phi_{\mathrm{EDL}}}{\partial Y_1^2} = -\rho_1 \quad \text{and} \quad \frac{\partial^2\Phi_{\mathrm{SCL}}}{\partial Y_2^2} = -z\rho_2, \tag{1}$$

and the continuity equations for electric current (that is obtained from the Nernst-Planck equations for positive and negative carriers in both fluid and solid domains),

$$\frac{\partial\rho_1}{\partial\tau} = \frac{\partial^2\rho_1}{\partial Y_1^2} - \rho_1 \quad \text{and} \quad \frac{t_w}{t_f}\frac{\partial\rho_2}{\partial\tau} = \frac{\partial^2\rho_2}{\partial Y_2^2} - \rho_2, \tag{2}$$

where τ is the dimensionless time normalized with the reference time $t_f = \lambda_{D1}^2/D_f$ and, in Eq. (2), $t_w = \lambda_{D2}^2/D_w$ (where D_f stands for the mass diffusivity for free charge carriers in liquid; for a dilute symmetric binary electrolyte, it is usually assumed that positive and negative free charge carriers have the same diffusivity, namely, $D_{p1} = D_{n1} = D_f$; in the solid wall, we also assume that both charge carriers have the save diffusivities, i.e., $D_{p2} = D_{n2} = D_w$). Such reference time t_f also can be expressed as $t_f = \varepsilon_0\varepsilon_f/\sigma_f = 1/\omega_D$, which denotes the charge relaxation time in the electrolytic solution and also can be viewed as the time that ions take to travel a Debye length by diffusion. ω_D is the Debye frequency of the electrolytic solution [24], and σ_f is the bulk electric conductivity of the electrolytic solution and can be formulated as $\sigma_f = 2n_{01}z^2e^2D_f/(k_BT)$. Similarly, the charge relaxation time t_w inside the semiconducting solid wall has the same physical interpretation as t_f.

On the solid surface, Φ_{EDL} and Φ_{SCL} satisfy the electrostatic boundary conditions [25]

$$\Phi_{\mathrm{EDL}} = \Phi_{\mathrm{SCL}}, \tag{3a}$$

and

$$\frac{\partial\Phi_{\mathrm{EDL}}}{\partial Y_1} - \beta\frac{\partial\Phi_{\mathrm{SCL}}}{\partial Y_2} = -q \quad \text{at} \quad Y_1 \ \text{or} \ Y_2 = 0, \tag{3b}$$

which, respectively, describe the continuity of the electric potential and the discontinuity of the electric displacement due to the presence of free charges at the interface between two different media. In Eq. (3), $\beta = (\varepsilon_w\lambda_{D1})/(\varepsilon_f\lambda_{D2})$, and q is the dimensionless free surface charge density that is scaled by $\varepsilon_0\varepsilon_f\Phi_0/\lambda_{D1}$.

Under the widely adopted assumptions—the solid surface is totally blocking, and there is no Faradaic reaction on the semiconducting surface, namely, the charge carrier fluxes cannot penetrate through the solid wall. The vanishing of normal components of the positive carriers flux and the

negative carrier flux inside both domains leads to the boundary conditions for ρ_1 and ρ_2, respectively, as

$$\frac{\partial \rho_1}{\partial Y_1} = -\frac{\partial \Phi_{\rm EDL}}{\partial Y_1} \quad \text{at} \quad Y_1 = 0, \tag{4a}$$

$$z\frac{\partial \rho_2}{\partial Y_2} = -\frac{\partial \Phi_{\rm SCL}}{\partial Y_2} \quad \text{at} \quad Y_2 = 0. \tag{4b}$$

At the outer edges of the EDL and the SCL, we impose the asymptotic matching conditions as

$$\Phi_{\rm EDL}|_{Y_1\to\infty} = \Phi_f\big|_{y\to 0} \quad \text{and} \quad \Phi_{\rm SCL}|_{Y_2\to-\infty} = \Phi_w|_{y\to 0}\,, \tag{5}$$

and the electroneutrality conditionsas

$$\rho_1 \to 0 \quad \text{as} \quad Y_1 \to \infty, \tag{6a}$$

$$\rho_2 \to 0 \quad \text{as} \quad Y_2 \to -\infty. \tag{6b}$$

We consider time periodic electrokinetic phenomena in an externally applied ac electric field with arbitrary wave forms, e.g., sinusoidal, triangular, rectangular, etc. The general time-dependent electric field is assumed to be continuous and to have a piecewise continuous first-order derivative over the period such that its value at $\tau = \tau + kT_0$ is identical for any integer k. Thus, a general periodic field quantity, X, can be expressed as a form in complex Fourier series, $X(\tau) = \sum_{k=-\infty}^{+\infty} X^{(k)}\exp(jk\Omega\tau)$, where $j = \sqrt{-1}$, Ω is the normalized frequency with respect to the Debye frequency ω_D of the electrolyte solution and it can be determined from $\Omega = 2\pi/T_0$. Here, $X^{(k)}$ represents the complex amplitude of the ambient field such that $X^{(-k)}$ denotes the complex conjugate of $X^{(k)}$. Thus, the aforementioned sum always renders a real function, and $X^{(k)}$ can be defined as $X^{(k)} = [\int X(\tau)\exp(-jk\Omega\tau)d\tau]/T_0$.

Due to its linearity, the present problem can be obtained as a superposition of an induced part satisfying the homogenous version of Eq. (3b), and an equilibrium part solely contributed by the surface charge density q. We focus on the induced part of the problem. Then, similar Fourier decompositions are assumed for the electric potentials ($\Phi_{\rm EDL}, \Phi_{\rm SCL}, \Phi_w$, and Φ_f) and the net charge densities ρ_i (i = 1,2) in terms of their corresponding complex amplitudes $\Phi_{\rm EDL}^{(k)}, \Phi_{\rm SCL}^{(k)}, \Phi_w^{(k)}$, $\Phi_f^{(k)}$ and $\rho_i^{(k)}$. Note that the component $k = 0$ corresponds to a steady dc electric forcing. The transformed problems resulting from Eq. (2) together with the boundary conditions given by Eqs. (4a) and (4b) yield the complex amplitudes for net charge densities$\rho_i^{(k)}$. Substituting these two results into the right-hand side of the transformed Eq. (1) and integrating twice with respect to Y_1 and Y_2, we can obtain

$$\Phi_{\rm EDL}^{(k)} = \frac{d\Phi_{\rm EDL}^{(k)}}{dY_1}\bigg|_{Y_1=0}\left[\left(1-\frac{1}{\gamma_1^2}\right)Y_1 - \frac{1}{\gamma_1^3}e^{-\gamma_1 Y_1}\right] + A_1, \tag{7a}$$

$$\Phi_{\rm SCL}^{(k)} = z\frac{d\Phi_{\rm SCL}^{(k)}}{dY_2}\bigg|_{Y_2=0}\left[\left(1-\frac{1}{\gamma_2^2}\right)Y_2 + \frac{1}{\gamma_2^3}e^{\gamma_2 Y_2}\right] + A_2, \tag{7b}$$

with $\gamma_1^2 = 1 + jk\Omega$ and $\gamma_2^2 = 1 + t_w jk\Omega/t_f$. At the outer edges of the two inner regions, i.e., $Y_1 \to \infty$ and $Y_2 \to -\infty$, the solutions given by Eqs. (7a) and (7b) are going to be matched with the solutions outside the EDL and SCL to determine the unknown coefficients. Hence, we have

$$\Phi_f^{(k)} = A_1 \quad \text{and} \quad \frac{d\Phi_f^{(k)}}{dy} = \frac{1}{\delta_1}\frac{d\Phi_{\rm EDL}^{(k)}}{dY_1}\bigg|_{Y_1=0}\left(1-\frac{1}{\gamma_1^2}\right) \quad \text{as} \quad y\to 0, \tag{8a}$$

$$\Phi_w^{(k)} = A_2 \quad \text{and} \quad \frac{d\Phi_w^{(k)}}{dy} = \frac{z}{\delta_2}\frac{d\Phi_{\rm SCL}^{(k)}}{dY_2}\bigg|_{Y_2=0}\left(1-\frac{1}{\gamma_2^2}\right) \quad \text{as} \quad y\to 0. \tag{8b}$$

The coefficient of the exponential term on the right-hand side of Eq. (7a) can be viewed as the complex amplitude for the effective induced ζ potential, that is, the potential drop across the EDL, i.e.,

$$\zeta_i^{(k)} = -\left(d\Phi_{\rm EDL}^{(k)}/dY_1|_{Y_1=0}\right)/\gamma_1^3 = -\delta_1\left(d\Phi_f^{(k)}/dy|_{y=0}\right)/\left[\gamma_1\left(\gamma_1^2-1\right)\right]. \tag{9}$$

Making use of Eqs. (8a) and (8b), we can eliminate A_1, A_2, $d\Phi_{\rm EDL}^{(k)}/dY_1|_{Y_1=0}$, and $d\Phi_{\rm SCL}^{(k)}/dY_2|_{Y_2=0}$ from the transformed boundary conditions Eq. (3) to obtain the following two equations:

$$\Phi_f^{(k)} - \Phi_w^{(k)} = \frac{d\Phi_f^{(k)}}{dy}\frac{\delta_1}{\gamma_1\left(\gamma_1^2-1\right)} + \frac{d\Phi_w^{(k)}}{dy}\frac{\delta_2}{\gamma_2\left(\gamma_2^2-1\right)} \quad \text{at} \quad y = 0, \tag{10a}$$

$$\delta_1\frac{\gamma_1^2}{\left(\gamma_1^2-1\right)}\frac{d\Phi_f^{(k)}}{dy} - \beta\delta_2\frac{\gamma_2^2}{\left(\gamma_2^2-1\right)}\frac{d\Phi_w^{(k)}}{dy} = 0 \quad \text{at} \quad y = 0. \tag{10b}$$

Equations (10a) and (10b) constitute the transformed version of the sought electrokinetic boundary conditions that directly connect the complex amplitudes of two bulk potentials ($\Phi_w^{(k)}$ and $\Phi_f^{(k)}$) across a semiconductor-electrolyte interface. These derived electrokinetic boundary conditions are the key results of the present analysis. They are applicable to the ac induced-charge electrokinetic flow over solids of any dielectric constant and conductivity in an electric field with arbitrary wave forms. For all finite values of β and t_w/t_f, the solution of the electrostatic problem consists of the simultaneous determination of the potentials $\Phi_f^{(k)}(\mathbf{r})$ and $\Phi_w^{(k)}(\mathbf{r})$ (wherein $\mathbf{r}$ denotes the position vector), which are harmonic (governed by Laplace's equation) within the respective fluid and solid domains, and satisfy the boundary conditions (10a) and (10b) on the surface of semiconducting solids [as well as the far-field conditions for $\Phi_f^{(k)}(\mathbf{r})$].

For conventional electrokinetic phenomena, solid walls are considered as perfect insulators, suggesting that both β and t_f/t_w are equal to zero. Then, it can be obtained from Eqs. (10a) and (10b) that there is no induced ζ potential (since, in this case, there is no electric field inside the solid, and $\Phi_f^{(k)} - \Phi_w^{(k)}$ is the effective induced ζ potential drop across the EDL), and the

bulk electrostatic potential inside the liquid domain satisfies the homogeneous Neumann condition, i.e., the electrically insulating condition ($d\Phi_f^{(k)}/dy = 0$).

For ideal dielectric objects in a dc electric field, the conductivity of the solids is zero (t_f /t_w = 0). Then, there is no SCL effect inside the solid, and the frequency of the external electric field is zero ($\Omega = 0$). Hence, Eqs. (10a) and (10b) can reduce to

$$\Phi_w^{(k)} + \frac{\varepsilon_w \lambda_{D_1}}{\varepsilon_f a}\frac{d\Phi_w^{(k)}}{dy} = \Phi_f^{(k)} \quad \text{at} \quad y = 0, \tag{11a}$$

$$\frac{d\Phi_f^{(k)}}{dy} = 0 \quad \text{at} \quad y = 0, \tag{11b}$$

which shows the Robin-type and Neumann-type boundary conditions of the steady electrostatic problems for the solid wall and the bulk liquid, respectively. The detailed derivation of Eqs. (11a) and (11b) was provided in Ref. [15] [see their Eqs. (2) and (9)].

To gain further physical insight into the two boundary conditions given in Eqs. (10a) and (10b), we substitute Eq. (9) into Eq. (10a) to obtain the charging equations for the EDL and the SCL, respectively, as

$$\frac{d\Phi_f^{(k)}}{dy} = -\frac{\zeta_i^{(k)}}{\delta_1}\left(\gamma_1^2 - 1\right)\gamma_1 \quad \text{at} \quad y = 0, \tag{12a}$$

$$\frac{d\Phi_w^{(k)}}{dy} = -\frac{\Phi_w^{(k)} - \Phi_f^{(k)} - \zeta_i^{(k)}}{\delta_2}\left(\gamma_2^2 - 1\right)\gamma_2 \quad \text{at} \quad y = 0. \tag{12b}$$

In Eqs. (12a) and (12b), the left-hand sides, respectively, represent the instantaneous Ohmic charging rates at the outer edges of the EDL and SCL, which are equal to the growth rates of their total induced charges shown on the right-hand sides of Eqs. (12a) and (12b). It is noted that $\Phi_w^{(k)} - \Phi_f^{(k)} - \zeta_i^{(k)}$ in Eq. (12b) denotes the potential drop across the SCL and is the counterpart of induced ζ potential $\zeta_i^{(k)}$ in the solid. If the EDL and SCL are to be considered as effective capacitors, we also can obtain frequency-dependent capacitances (in dimensional form) for the EDL as $\varepsilon_0\varepsilon_f\gamma_1/\lambda_{D1}$ and the SCL as $\varepsilon_0\varepsilon_w\gamma_2/\lambda_{D2}$. Therefore, the present paper provides a rigorous alternative to the widely used equivalent *RC*-circuit models for the EDL in ACEK phenomena, where the capacitance of EDL reads $\varepsilon_0\varepsilon_f/\lambda_{D1}$, which is independent of frequency [1,24,26]. Also shown in the above conditions is the parameter $\beta = (\varepsilon_w\lambda_{D1})/(\varepsilon_f\lambda_{D2})$, which, based on the equivalent *RC*-circuit model, represents the ratio of the capacitance of the SCL $\varepsilon_0\varepsilon_w/\lambda_{D2}$ and that of the EDL $\varepsilon_0\varepsilon_f$ /λ_{D1}. From this analogy, it is anticipated that, when $\beta \gg 1$, the difference $\Phi_w^{(k)} - \Phi_f^{(k)}$, effectively representing the complex amplitude of induced ζ potential $\zeta_i^{(k)}$, becomes of comparable magnitude as $\Phi_f^{(k)}$. In the limit case of $\beta \to \infty$ (i.e., a perfectly polarizable solid), $\Phi_w^{(k)} = 0$ (also $d\Phi_w^{(k)}/dy = 0$ since the electric field does not exist inside such a perfectly polarizable solid) and our derived Eq. (12a) then precisely reduce to the macroscale model presented in Ref. [6] [see their Eqs. (7.48) and (7.50)].

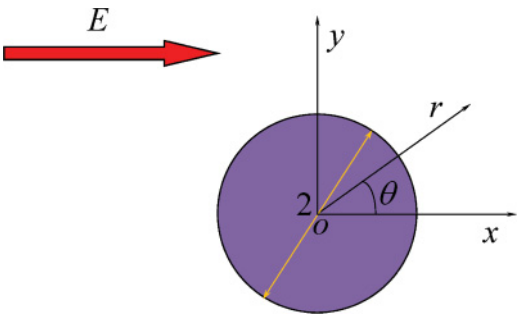

FIG. 2. (Color online) A semiconducting cylinder immersed in an unbounded electrolyte solution is under an ac electric field with a sinusoidal wave form. The external electric field E is applied along the x direction. Coordinates are normalized with respect to the radius of cylinder (R), and the electric field strength is normalized with respect to Φ_0/R.

III. ACEK FLOW AROUND A SEMICONDUCTIVE CYLINDER

In this section, we will demonstrate the implementation of the effective boundary conditions derived in Sec. II for an ac induced-charge flow around a semiconducting cylinder (see Fig. 2). Such a semiconducting cylinder with a radius of R immersed in an electrolyte solution is put (electrically floating) in an ac electric field of sinusoidal wave form, expressed as $E = \mathrm{Re}[E_0\exp(j\Omega\tau)]$ with Re( ) denoting the real part of the complex number. Then, the EDL inside the liquid domain and the SCL inside the solid domain develop near the semiconducting surface. It was already mentioned that the complex amplitudes of potentials inside the bulk electroneutral liquid and solid domains, Φ_f and Φ_w, were all governed by Laplace's equation. The boundary conditions connecting these two domains are described by Eqs. (10a) and (10b), which, in polar coordinates, can be reformulated as

$$\Phi_f - \Phi_w = \frac{\partial\Phi_f}{\partial r}\frac{\delta_1}{\gamma_1\left(\gamma_1^2 - 1\right)} + \frac{\partial\Phi_w}{\partial r}\frac{\delta_2}{\gamma_2\left(\gamma_2^2 - 1\right)} \quad \text{at} \quad r = 1, \tag{13a}$$

$$\delta_1\frac{\gamma_1^2}{\left(\gamma_1^2 - 1\right)}\frac{\partial\Phi_f}{\partial r} - \beta\delta_2\frac{\gamma_2^2}{\left(\gamma_2^2 - 1\right)}\frac{\partial\Phi_w}{\partial r} = 0 \quad \text{at} \quad r = 1. \tag{13b}$$

For the *RC*-circuit model, the effective electric boundary conditions can be formulated as

$$\Phi_f - \Phi_w = \frac{\partial\Phi_f}{\partial r}\frac{\delta_1}{\left(\gamma_1^2 - 1\right)} + \frac{\partial\Phi_w}{\partial r}\frac{\delta_2}{\left(\gamma_2^2 - 1\right)} \quad \text{at} \quad r = 1, \tag{14a}$$

$$\delta_1\frac{\gamma_1^2}{\left(\gamma_1^2 - 1\right)}\frac{\partial\Phi_f}{\partial r} - \beta\delta_2\frac{\gamma_2^2}{\left(\gamma_2^2 - 1\right)}\frac{\partial\Phi_w}{\partial r} = 0 \quad \text{at} \quad r = 1, \tag{14b}$$

which are to be compared against our present model in Eq. (13). For simplicity, the following derivations are carried out only

for the boundary conditions presented in Eq. (13) but not for the boundary conditions in Eq. (14).

In addition, we also need a far-field condition for Φ_f,

$$\Phi_f = -E_0 x = -E_0 r\cos\theta \quad \text{as} \quad r \to \infty. \tag{15}$$

In Eqs. (13)–(15), the potentials, electric field strength, and radial coordinate, respectively, are normalized with respect to Φ_0,Φ_0/R, and R. Referring to the definitions of two electrokinetic parameters, δ_1 and δ_2, in Sec. II, one can write $\delta_1 = \lambda_{D1}/R$ and $\delta_2 = \lambda_{D2}/R$ in this case. For the given sinusoidal ac electric field, $\gamma_1^2 = 1 + j\Omega$ and $\gamma_2^2 = 1 + jt_w\Omega/t_f$.

The electrostatic potentials satisfy Laplace's equation in both bulk liquid and solid domains, and the solutions for complex amplitudes of the potential inside the bulk electrolyte domain Φ_f and inside the bulk semiconductive cylinder Φ_w are assumed as [27]

$$\Phi_f = -E_0\cos\theta\left(r + \frac{A}{r}\right), \tag{16a}$$

$$\Phi_w = -BE_0 r\cos\theta. \tag{16b}$$

Substitution of Eqs. (16a) and (16b) into Eqs. (13a) and (13b) gives two expressions for

$$A = 1 - \frac{2\beta G_2\gamma_2^3}{G_1\gamma_1^3(1+G_2) + \beta G_2\gamma_2^3(1+G_1)}, \tag{17a}$$

$$B = \frac{2G_1\gamma_1^3}{G_1\gamma_1^3(1+G_2) + \beta G_2\gamma_2^3(1+G_1)}, \tag{17b}$$

where G_1 and G_2 are two complex groups related to the liquid domain and the solid domain, respectively,

$$G_1 = \frac{\delta_1}{\gamma_1\left(\gamma_1^2 - 1\right)}, \tag{18a}$$

$$G_2 = \frac{\delta_2}{\gamma_2\left(\gamma_2^2 - 1\right)}. \tag{18b}$$

Furthermore, the tangential electric field strength on the semiconducting surface reads

$$E_\theta = -\frac{1}{r}\frac{\partial\Phi_f}{\partial\theta} = -E_0\sin\theta(1+A) \quad \text{at} \quad r = 1. \tag{19}$$

In this particular case, the complex amplitude of the induced ζ potential defined by Eq. (9) can be formulated as

$$\zeta_i = -\frac{\partial\Phi_f}{\partial r}\frac{\delta_1}{\gamma_1\left(\gamma_1^2 - 1\right)} = G_1(1-A)E_0\cos\theta \quad \text{at} \quad r = 1. \tag{20}$$

It is evident from Eq. (20), that the induced ζ potential is linearly proportional to the external electric field strength. For a conducting cylinder with ideal polarizability under a dc forcing, i.e., $\beta \to \infty$ and $\Omega \to 0$, we can obtain the induced ζ potential as

$$\zeta_i = 2E_0\cos\theta, \tag{21}$$

which is identical to the result given by Eq. (3.5) in Ref. [6].

Utilizing the well-known Smoluchowski equation, the ac induced-charge electroosmotic slip velocity on the surface of such semiconducting cylinder can be determined by

$$\mathbf{u}_s = U_0 E_0^2\sin\theta\cos\theta\,\widehat{\boldsymbol{\theta}}, \tag{22}$$

where $\widehat{\boldsymbol{\theta}}$ denotes the unit vector along the azimuthal direction, and U_0 can be determined as

$$U_0 = \mathrm{Re}[G_1(1-A)\exp(j\Omega\tau)]\mathrm{Re}[(1+A)\exp(j\Omega\tau)]. \tag{23}$$

The Smoluchowski slip velocity approach is strictly valid when the induced EDL is in quasiequilibrium ($\Omega \ll 1$), however, it was also shown to be a good approximation even for relatively high frequencies ($\Omega \sim 1$) [28].

Once the slip velocity $\mathbf{u}_s$ is obtained from the above solution of the electrostatic problem, we can now proceed to solve the flow field around the semiconducting cylinder. Because the Reynolds number is very small in microfluidics, the flow of the bulk electroneutral fluid is governed by the dimensionless continuity equation and the Stokes equation [29],

$$\nabla\cdot\mathbf{u} = 0 \quad \text{and} \quad -\nabla p + \nabla^2\mathbf{u} = 0, \tag{24}$$

respectively, which are subjected to the slip boundary condition

$$\mathbf{u} = \mathbf{u}_s \quad \text{at} \quad r = 1, \tag{25}$$

and the far-field boundary condition

$$\mathbf{u} = 0 \quad \text{as} \quad r \to \infty, \tag{26}$$

where $\mathbf{u}$ and p represent the fluid velocity vector and the pressure, respectively, and they are normalized by $\varepsilon_0\varepsilon_f\Phi_0^2/(\mu R)$ and $\varepsilon_0\varepsilon_f\Phi_0^2/R^2$, respectively.

It is convenient to make use of the stream function formulation to solve such a hydrodynamic problem. First, we can express the radial (u_r) and azimuthal (u_θ) velocity components in terms of the stream function ψ,

$$u_r = \frac{1}{r}\frac{\partial\psi}{\partial\theta} \text{ and } u_\theta = -\frac{\partial\psi}{\partial r}, \tag{27}$$

where the stream function is normalized with respect to $\varepsilon_0\varepsilon_f\Phi_0^2/\mu$.

Then, substituting Eq. (27) into Eq. (24), we can obtain the following biharmonic equation that governs the flow field:

$$\nabla^2(\nabla^2\psi) = 0, \tag{28}$$

where operator ∇^2 in the polar coordinate can be expressed as

$$\nabla^2 = \frac{1}{r}\frac{\partial}{\partial r}\left(r\frac{\partial}{\partial r}\right) + \frac{1}{r^2}\frac{\partial^2}{\partial\theta^2}. \tag{29}$$

The boundary conditions given by Eqs. (25) and (26) can be transformed to

$$\frac{1}{r}\frac{\partial\psi}{\partial\theta} = 0 \text{ and } \frac{\partial\psi}{\partial r} = -U_0 E_0^2\sin\theta\cos\theta \quad \text{at} \quad r = 1, \tag{30}$$

as well as the far-field boundary conditions

$$\frac{1}{r}\frac{\partial\psi}{\partial\theta} = 0 \text{ and } -\frac{\partial\psi}{\partial r} = 0 \quad \text{as} \quad r \to \infty. \tag{31}$$

Squires and Bazant [6] derived the solutions for the fluid motion around a perfectly polarizable cylinder immersed in an

electrolyte solution in a dc field (see their Table 1). By analogy, we can find the stream function and the corresponding velocity components of the fluid flow outside the semiconducting cylinder to be

$$\psi = \frac{1-r^2}{4r^2} U_0 E_0^2 \sin 2\theta, \tag{32a}$$

$$u_r = \frac{1-r^2}{2r^3} U_0 E_0^2 \cos 2\theta, \tag{32b}$$

$$u_\theta = \frac{1}{2r^3} U_0 E_0^2 \sin 2\theta, \tag{32c}$$

which reveal that the flow field scales nonlinearly with respect to the external electric field strength. This feature differs from classic electrokinetic flows over insulating surfaces where the flow field is linearly proportional to the external electric field strength. Again, for the limiting case of an ideally polarizable cylinder under the dc forcing, Eqs. (32a)–(32c) are shown to be identical to those results given in Ref. [6],

$$\psi = \frac{1-r^2}{r^2} E_0^2 \sin 2\theta, \tag{33a}$$

$$u_r = \frac{2(1-r^2)}{r^3} E_0^2 \cos 2\theta, \tag{33b}$$

$$u_\theta = \frac{2}{r^3} E_0^2 \sin 2\theta. \tag{33c}$$

IV. RESULTS AND DISCUSSION

Calculations are performed by using the derivations presented in Sec. III to show the induced-charge electrokinetic flow patterns around a semiconducting cylinder under various ac phases. For simplicity, we first consider a special cylindrical conductor with ideal polarizability ($\beta \to \infty$). The stream

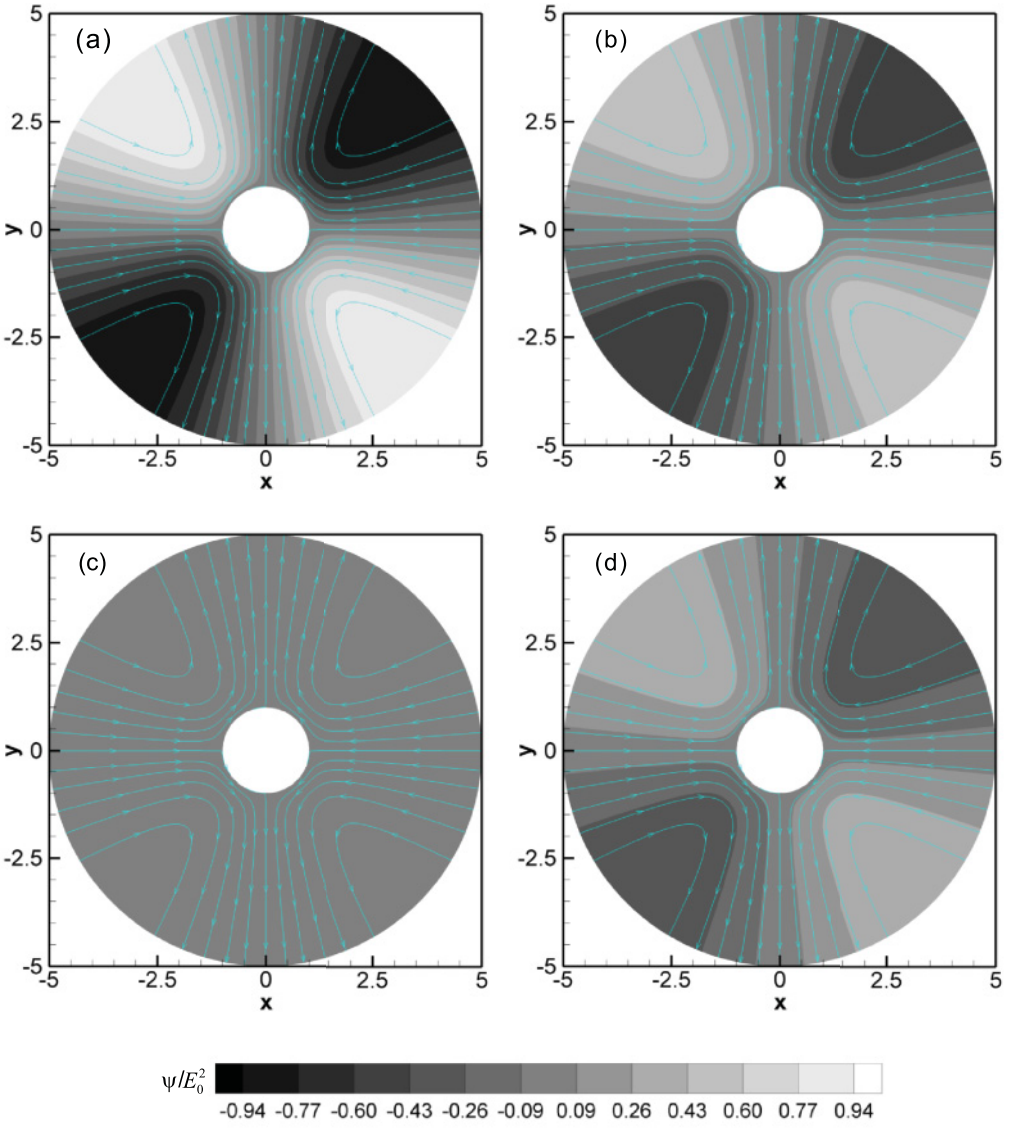

FIG. 3. (Color online) Contours for the stream function of an ac induced-charge electrokinetic flow at four different ac phases for the case of a conducting cylinder with perfect polarizability ($\beta \to \infty$): (a) $\Omega\tau = 0$, (b) $\Omega\tau = \pi/4$, (c) $\Omega\tau = \pi/2$, and (d) $\Omega\tau = 3\pi/4$. The arrowed lines are stream lines. In the calculations, the electrokinetic parameter is $\delta_1 = 1/100$, and the frequency is $\Omega = 0.001$.

function contours (normalized with respect to E_0^2) of induced-charge electrokinetic flow at four different ac phases are plotted in Fig. 3. In the calculation, the reference zero stream function is chosen on the cylinder surface. Then, the stream function value at a given point in the flow field denotes the volumetric flow rate through a line connecting that point and the semiconducting surface. Usually, the magnitude of the stream function value can be seen as a measure of the flow strength. It is evident from Fig. 3(a) that the flow is strongest at the phase $\Omega\tau = 0$. Basic flow field involves four vortices symmetric with respect to both x and y axes. These flow circulations are the consequence of induced slip velocities on four segments of the cylinder surface, which all direct toward the line $x = 0$. With time evolving, both the external field strength and the induced ζ potential decrease, which then leads to a reduction in the flow strength [see the phase $\Omega\tau = \pi/4$ shown in Fig. 3(b)]. For the phase $\Omega\tau = \pi/2$ in Fig. 3(c), although the external electric field further decreases to zero, the tangential electric field strength on the cylinder surface given by Eq. (19) and the induced ζ potential given by Eq. (20) are not zero due to the essential phase lags among these two and the external field. Consequently, the fluid slip velocity on the cylinder surface and, thus, the weak circulations still persist. After the phase $\Omega\tau = \pi/2$, the external electric field changes its direction, and the local induced ζ potential on the cylinder surface also reverses its sign. Thus, the direction of the induced slip velocity (as a product of the tangential electric field strength and the induced ζ potential) on cylinder surface still remains the same as that in the first half period (namely, $\Omega\tau$ from 0 to $\pi/2$) and so does the direction of flow circulations. With the magnitude of electric field strength increasing, the flow becomes intensified as shown in Fig. 3(d) for the phase of $\Omega\tau = 3\pi/4$. Until the phase $\Omega\tau = \pi$ (not shown here), the flow is enhanced to reach the same situation as for the phase $\Omega\tau = 0$. Finally, it is also worth mentioning that the frequency of induced-charge flow oscillation is doubled to 2Ω since both driving electric field and induced ζ potential oscillate at the frequency of Ω.

If the case of an ideally polarized cylinder under the dc forcing is taken as a reference, the induced-charge flow field around a semiconducting cylinder can be found by multiplying the solutions given by Eq. (33) with a scale factor of $U_0/4$. This scale factor is important since the parameters affecting the dynamics of the induced-charge oscillating flow around the semiconducting cylinder are included in such a factor, such as the period, the amplitude, and the phase. Figure 4 characterizes the dependence of $U_0/4$ on the ac phase for a semiconducting cylinder under various frequencies of the external field (Ω) and ratios of the free charge relaxation times (t_w/t_f). It is seen that the amplitude of the flow oscillation increases with decreasing Ω or t_w/t_f. It is also noted that the phase lag between the induced-charge flow and the external electric field also reduces with the decrease in Ω or t_w/t_f. These features can be interpreted as follows: when Ω is low, there is sufficient time for free charge carriers to diffuse into the EDL and SCL to charge them up. On the other hand, with decreasing t_w/t_f, the cylinder becomes more conducting, and the free charges inside such a semiconducting cylinder can respond quickly to form the SCL, which effectively represents a surface charge on the cylinder surface.

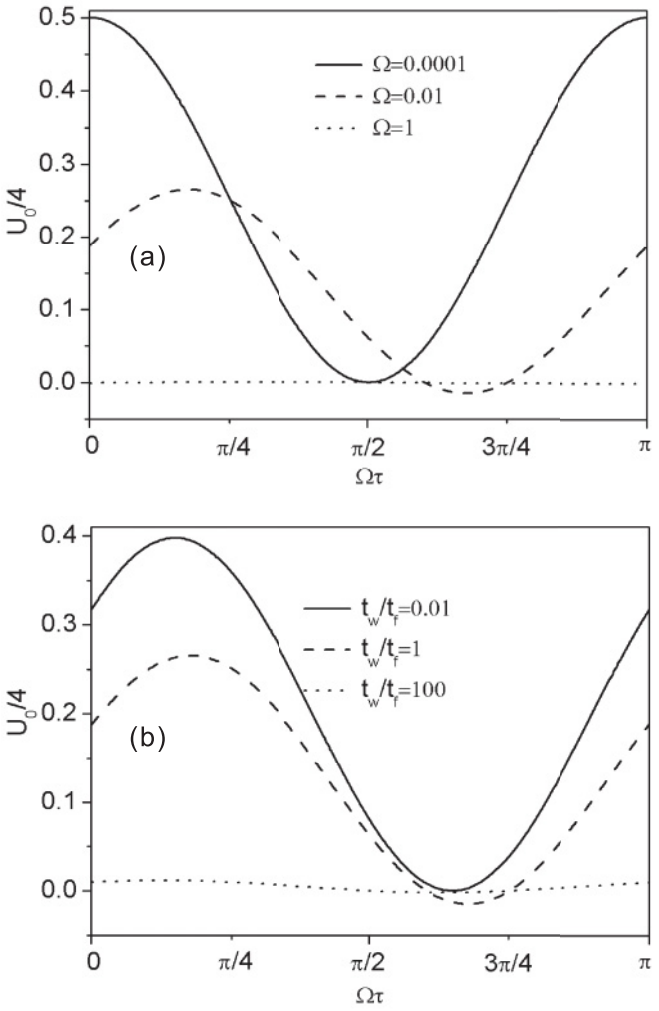

FIG. 4. Variation of $U_0/4$ for an ac induced-charge electrokinetic flow around a semiconducting cylinder with an ac phase angle [here, the expression for U_0 is given by Eq. (23)]. (a) Dependence of $U_0/4$ on the frequency of the ac field, Ω, when $t_w/t_f = 1.0$. (b) Dependence of $U_0/4$ on the free charge relaxation time ratio t_w/t_f, when $\Omega = 0.01$. In all calculations, $\beta = 1$ and $\delta_1 = \delta_2 = 1/100$ are chosen.

In addition, it is known that the *RC*-circuit model is widely used in the literature. To illustrate the difference between our present model and the conventional *RC*-circuit model, the ratio of the complex amplitude for the induced ζ potential obtained from our model (ζ_i) to that predicted from the *RC* model ($\zeta_{i,RC}$) is presented in Fig. 5. ζ_i and $\zeta_{i,RC}$ are evaluated by using boundary conditions (13) and (14), respectively. Since $\zeta_i/\zeta_{i,RC}$ is a complex number, its modulus represents the ratio of the magnitude of the induced ζ potential evaluated from our model to that evaluated from the *RC* model, and its argument represents the phase lag between our model and the *RC* model. It is noted that our model and the *RC* model become identical only in the case of dc electric forcing ($\Omega \to 0$). However, as the frequency of applied field increases, our model predicts smaller induced ζ potentials, and the phase lag between our model and the *RC* model becomes larger. Similarly, it also can be readily found that both the tangential electric field strength given by Eq. (19) and the resultant Smoluchowski slip velocity given by Eq. (22) are smaller than those predicted

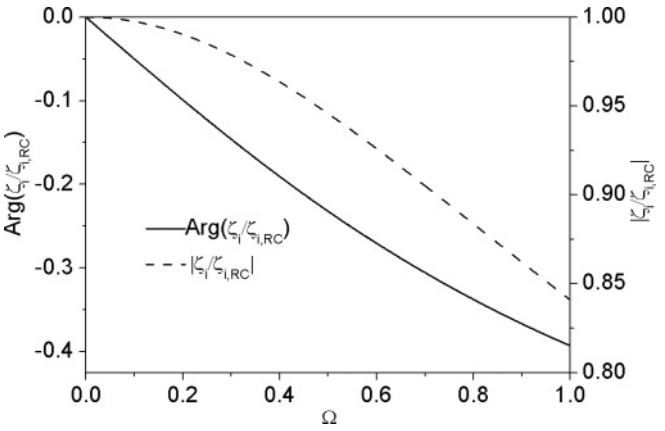

FIG. 5. Ratio of the complex amplitude of the induced ζ potentials predicted by the present model (ζ_i) to that predicted by the conventional *RC*-circuit model ($\zeta_{i,RC}$)for the case of a conducting cylinder with perfect polarizability ($\beta \to \infty$) and $\delta_1 = 1/1000$. The left vertical axis represents the argument for the complex ratio $\zeta_i/\zeta_{i,RC}$, and the right vertical axis represents the corresponding modulus.

by the *RC* model. As pointed out in a review paper by Bazant *et al*. [30], the *RC* model was shown to overestimate existing experimental results for the ICEK flow velocity. Therefore, the model presented in this paper could reduce such a discrepancy to some extent.

Considering the fact that the SCL is actually an equivalent EDL in the solid, the derived effective boundary conditions can be extended to describe dynamic behavior of an interface between two immiscible electrolyte solutions under ac electric forcing. Interfaces between two immiscible electrolyte solutions are widely used for biomimetics, catalysis, surface cleaning, and assembly of nanoparticle arrays [31,32]. Monroe and co-workers [33,34] investigated the behavior of an interface between two immiscible electrolyte solutions under the dc forcing, and they pointed out that two EDLs forming near the interface between two immiscible electrolyte solutions play an essential role. Another potential application of presented boundary conditions is to modify the classic dielectrophoresis theory for semiconducting particles in electrolyte solutions. It is known that EDL and SCL are not considered in the conventional theories of dielectrophoresis. Usually, an assumption of the continuity in both electric potential and electric displacement should be made when deriving the dielectrophoretic force and torque acting on a particle. However, this assumption is not valid for a semiconducting particle in which the SCL of finite thickness develops. Obviously, in this case, the continuity of electric potential does not hold anymore [see Eq. (10a)] due to the charging of EDL and SCL. Then, the local electric field around the particle should be modified accordingly. Ultimately, the effective dipole moment and, therefore, the dielectrophoretic force and torque on a semiconducting particle need to be modified by taking the dynamic charging of EDL and SCL into account. Although some researchers [22,35–37] noticed this problem and already addressed the EDL charging effect on dielectrophoretic force, the SCL effects have yet to be addressed. Furthermore, no one has ever provided any simple formulas for the dielectrophoretic force and torque on a spherical particle to include both EDL and SCL effects. With our derived effective boundary conditions, it can be expected that the modification of conventional dielectrophoretic theory can be included in a modified Clausius-Mossoti factor. This will be our next effort.

V. SUMMARY

To conclude, we have derived effective electric boundary conditions for ACEK phenomena around floating semiconducting solids in an ac electric field with arbitrary wave forms. The general electric boundary conditions take the contributions from both the electrical polarization and the electrical conduction to induced ζ potentials into account. We have demonstrated that our general boundary conditions can recover two well-known limiting cases, (i) the conventional electrokinetic phenomena with perfect insulating surfaces and (ii) the induced-charge electrokinetic phenomena with perfectly polarizable surfaces. The effective electric boundary conditions also allow us to analyze ACEK phenomena with induced EDL and SCL effects without the need of resolving trivial details of the EDL and SCL.

A case study of the ac induced-charge electrokinetic flow around a semiconducting cylinder is presented to demonstrate the implementation of the derived boundary conditions. Our analyses show that four flow circulations are induced around the semiconducting cylinder. Furthermore, the intensity of these circulations can be modulated by adjusting the parameters associated with the EDL and SCL. Particularly, when decreasing the frequency of the applied electric field (Ω) or the ratio of the free charge relaxation times (t_w/t_f), the amplitude of the induced-charge flow oscillation increases, and the phase lag between the induced-charge electrokinetic flow and the external electric field decreases. In addition, a comparison between our present model and the conventional *RC*-circuit model shows that the *RC* model predicts larger values for the induced ζ potential, and, thus, stronger induced-charge electrokinetic flows. This could explain the finding reported by some studies that the *RC* model usually overestimates the experimental data of induced-charge electrokinetic flows.

ACKNOWLEDGMENT

The authors gratefully acknowledge the financial support from the Ministry of Education of Singapore to C.Y. (Grant No. MOE2009-T2-2-102).

[1] A. Ramos, H. Morgan, N. G. Green, and A. Castellanos, J. Colloid Interface Sci. **217**, 420 (1999).
[2] M. P. Hughes, Nanotechnology **11**, 124 (2000).
[3] H. Morgan and N. G. Green, *AC Electrokinetics: Colloids and Nanoparticles* (Research Studies Press, Philadelphia, PA, 2003).
[4] N. I. Gamayunov, V. A. Murtsovkin, and A. S. Dukhin, Colloid J. USSR **48**, 197 (1986).
[5] V. A. Murtsovkin, Colloid J. **58**, 341 (1996).
[6] T. M. Squires and M. Z. Bazant, J. Fluid Mech. **509**, 217 (2004).

[7] M. M. Gregersen, F. Okkels, M. Z. Bazant, and H. Bruus, New J. Phys. **11**, 075019 (2009).
[8] Z. Wu and D. Li, Electrochim. Acta **53**, 5827 (2008).
[9] C. K. Harnett, J. Templeton, K. A. Dunphy-Guzman, Y. M. Senousy, and M. P. Kanouff, Lab Chip **8**, 565 (2008).
[10] F. C. Leinweber, J. C. T. Eijkel, J. G. Bomer, and A. Van Den Berg, Anal. Chem. **78**, 1425 (2006).
[11] F. O. Mavré, R. K. Anand, D. R. Laws, K.-F. Chow, B.-Y. Chang, J. A. Crooks, and R. M. Crooks, Anal. Chem. **82**, 8766 (2010).
[12] T. M. Squires and M. Z. Bazant, J. Fluid Mech. **560**, 65 (2006).
[13] S. Gangwal, O. J. Cayre, M. Z. Bazant, and O. D. Velev, Phys. Rev. Lett. **100**, 058302 (2008).
[14] G. Yossifon, I. Frankel, and T. Miloh, Phys. Fluids **19**, 068105 (2007).
[15] C. Zhao and C. Yang, Phys. Rev. E **80**, 046312 (2009).
[16] G. Yossifon, I. Frankel, and T. Miloh, J. Fluid Mech. **620**, 241 (2009).
[17] A. J. Pascall and T. M. Squires, Phys. Rev. Lett. **104**, 088301 (2010).
[18] J. Bardeen, Phys. Rev. **71**, 717 (1947).
[19] B. V. King and F. Freund, Phys. Rev. B **29**, 5814 (1984).
[20] J. O. M. Bockris, A. K. N. Reddy, and M. E. Gamboa-Aldeco, *Modern Electrochemistry 2A: Fundamentals of Electrodics* (Kluwer Academic, New York, 2002).
[21] J. O. M. Bockris and A. K. N. Reddy, *Modern Electrochemistry 2B: Electrodics in Chemistry, Engineering, Biology, and Environmental Science* (Kluwer Academic, New York, 2004).
[22] T. N. Swaminathan and H. H. Hu, Mech. Res. Commun. **36**, 46 (2009).
[23] C. Zhao and C. Yang, Electrophoresis **32**, 629 (2011).
[24] A. Ajdari, Phys. Rev. E **61**, R45 (2000).
[25] D. T. Paris and F. K. Hurd, *Basic Electromagnetic Theory* (McGraw-Hill, New York, 1969).
[26] A. Castellanos, A. Ramos, A. González, N. G. Green, and H. Morgan, J. Phys. D **36**, 2584 (2003).
[27] A. P. S. Selvadurai, *Partial Differential Equations in Mechanics: Fundamentals, Laplace's Equation, Diffusion Equation, Wave Equation* (Springer, Berlin, 2000).
[28] A. Ramos, A. González, P. García-Sánchez, and A. Castellanos, J. Colloid Interface Sci. **309**, 323 (2007).
[29] H. Zhao and H. H. Bau, Phys. Rev. E **75**, 066217 (2007).
[30] M. Z. Bazant, M. S. Kilic, B. D. Storey, and A. Ajdari, Adv. Colloid Interface Sci. **152**, 48 (2009).
[31] B. Su, J.-P. Abid, D. J. Fermín, H. H. Girault, H. Hoffmannová, P. Krtil, and Z. Samec, J. Am. Chem. Soc. **126**, 915 (2003).
[32] H. H. Girault and D. J. Schiffrin, in *Electroanalytical Chemistry*, edited by A. J. Bard (Dekker, New York, 1985), Vol. 15, p. 1.
[33] C. W. Monroe, L. I. Daikhin, M. Urbakh, and A. A. Kornyshev, Phys. Rev. Lett. **97**, 136102 (2006).
[34] C. W. Monroe, M. Urbakh, and A. A. Kornyshev, J. Electrochem. Soc. **156**, P21 (2009).
[35] S. Basuray and H.-C. Chang, Phys. Rev. E **75**, 060501 (2007).
[36] H. Zhao and H. H. Bau, J. Colloid Interface Sci. **333**, 663 (2009).
[37] P. D. Hoffman and Y. Zhu, Appl. Phys. Lett. **92**, 224103 (2008).